


In-plane microvortices micromixer-based AC electrothermal for testing drug induced death of tumor cells

Cite as: Biomicrofluidics **10**, 064102 (2016); <https://doi.org/10.1063/1.4967455>

Submitted: 08 August 2016 . Accepted: 28 October 2016 . Published Online: 14 November 2016

Qi Lang, Yukun Ren,  Divia Hobson, Ye Tao, Likai Hou, Yankai Jia, Qingming Hu, Jiangwei Liu, Xin Zhao, and Hongyuan Jiang



View Online



Export Citation



CrossMark

ARTICLES YOU MAY BE INTERESTED IN

[Dielectrophoretic separation with a floating-electrode array embedded in microfabricated fluidic networks](#)

Physics of Fluids **30**, 112003 (2018); <https://doi.org/10.1063/1.5054800>

[On utilizing alternating current-flow field effect transistor for flexibly manipulating particles in microfluidics and nanofluidics](#)

Biomicrofluidics **10**, 034105 (2016); <https://doi.org/10.1063/1.4949771>

[Particle rotational trapping on a floating electrode by rotating induced-charge electroosmosis](#)

Biomicrofluidics **10**, 054103 (2016); <https://doi.org/10.1063/1.4962804>



Biophysics Reviews

First Articles Now Online!

READ NOW >>>



In-plane microvortices micromixer-based AC electrothermal for testing drug induced death of tumor cells

Qi Lang,^{1,2} Yukun Ren,^{1,3,a)} Divia Hobson,⁴ Ye Tao,¹ Likai Hou,¹ Yankai Jia,¹ Qingming Hu,¹ Jiangwei Liu,¹ Xin Zhao,^{4,a)} and Hongyuan Jiang^{1,3,a)}

¹School of Mechatronics Engineering, Harbin Institute of Technology, Harbin 150001, China

²Institute of Biomedicine and Biotechnology, Shenzhen Institutes of Advanced Technology, Chinese Academy of Sciences, Shenzhen 518055, China

³State Key Laboratory of Robotics and System, West Da-zhi Street 92, Harbin 150001, China

⁴Interdisciplinary division of Biomedical Engineering, the Hong King Polytechnique University, Hunghom, Hong Kong, China

(Received 8 August 2016; accepted 28 October 2016; published online 8 November 2016)

Herein, we first describe a perfusion chip integrated with an AC electrothermal (ACET) micromixer to supply a uniform drug concentration to tumor cells. The in-plane fluid microvortices for mixing were generated by six pairs of reconstructed novel ACET asymmetric electrodes. To enhance the mixing efficiency, the novel ACET electrodes with rotating angles of 0°, 30°, and 60° were investigated. The asymmetric electrodes with a rotating angle of 60° exhibited the highest mixing efficiency by both simulated and experimental results. The length of the mixing area is 7 mm, and the mixing efficiency is 89.12% (approximate complete mixing) at a voltage of 3 V and a frequency of 500 kHz. The applicability of our micromixer with electrodes rotating at 60° was demonstrated by the drug (tamoxifen) test of human breast cancer cells (MCF-7) for five days, which implies that our ACET in-plane microvortices micromixer has great potential for the application of drug induced rapid death of tumor cells and mixing of biomaterials in organs-on-a-chip systems. *Published by AIP Publishing*. [<http://dx.doi.org/10.1063/1.4967455>]

I. INTRODUCTION

Organs-on-a-chip is an outstanding microfluidic platform for drug and vaccine screening applications as well as *in-vitro* disease models.¹⁻⁴ Pharmaceutical testing currently conducted through poorly predictive animal experiments and dangerous clinical tests will be gradually phased out and replaced by organs-on-a-chip systems.^{5,6} These chip systems are connected by microfluidic channels that are assembled according to the organ networks in the human body to mimic the dynamic *in vivo* environment.⁷⁻⁹ Laminar flows in these microfluidic channels present a challenge for effective diffusional mixing of the culture medium, metabolites, drugs, or other biological signals from multi-organ chips.^{10,11} As a consequence of poor mixing, the cells, tissues, or sensors in organs-on-a-chip systems will present inexact results in drug or vaccine testing. Therefore, a rapid micromixer is highly desired for integration into organs-on-a-chip systems.

In keeping with the principle of mixing, micromixers can be classified into passive^{12,13} and active mixers.^{14,15} Of the various micromixers reported in the past years, passive mixers, which have included lamination,^{16,17} intersecting or disturbing channels,^{18,19} and droplet-based platforms,^{20,21} have not required energy input or moving parts. Passive mixers are, however, difficult to integrate into organs-on-a-chip systems due to the complexity of their structures. Active mixers enhance the mixing performance using some form of external energy supply, which can include

^{a)}Authors to whom correspondence should be addressed. Electronic addresses: rykhit@hit.edu.cn; xinzhao666666@163.com; and jhy_hit@hit.edu.cn.

the electric,^{22,23} magnetic,²⁴ and acoustic²⁵ fields in addition to others. Of late, theoretical and experimental studies on AC electrokinetics^{26–28} have extended to AC electroosmosis (ACEO)^{29,30} and AC electrothermal (ACET).³¹ The mechanism of ACEO is not effective in the high-conductivity fluid and unsuitable for the fluids in organs-on-a-chip platforms. Furthermore, in the high-conductivity fluid or cell culture medium, the layer of induced mobile charges becomes immensely compressed and loses its drag in the fluid.³² ACET emerges from the interaction of an electric field with a temperature gradient and is especially suited for manipulating high conductivity fluids.³² Although efficient ACET mixers were reported, several issues are remained to be addressed for the application in organs-on-a-chip systems. Ng *et al.*³³ reported a micromixer that can be operated from the ACEO ($\sigma = 1$ mS/m) to the ACET ($\sigma = 500$ mS/m) with the voltage of 20 V. Sasaki *et al.*²³ designed a pair of coplanar electrodes with a sinusoidal interelectrode gap to mix the fluids ($\sigma = 1.29$ S/m) with the voltage of 30 V. Wu *et al.*³⁴ used ACET 3-D electrodes to mix the fluids ($\sigma = 0.2$ – 1 S/m) with the voltage of 42–51.75 V. The electric conductivity of cell culture medium is around 1.7 S/m, which is beyond the upper limit of the previous study of the ACET micromixer. Huge joule heat will be generated in cell culture medium with the high voltages in the above studies ($V = 20$ – 51.75 V), which will damage the cells or destroy some of the protein in the culture medium. In a previous study,³⁵ we reported on the development of a circulatory pumping chip for cell culture utilizing ACET with low voltage ($V = 3$ V). The cell culture medium was pumped by an ACET asymmetric electrode array, while two types of human cells, embryonic kidney (HEK293T) and colon carcinoma (SW620), grew well in the device for more than 72 h without experiencing Joule heating from ACET flow or electrical damage from the electrodes. This is a conventional asymmetric electrode array where ACET flow moves from the narrow electrode toward the broad one^{26,36} (Fig. 1(a)). If the asymmetric electrode array was restructured, the ACET flow could achieve greater mixing capability and overall functionality.

In this paper, we report a micromixer with novel ACET asymmetric electrode array generated in-plane microvortices (Fig. 1(b)). The upper half and lower half of the paired electrodes simultaneously produce opposite ACET flows. As a result, the anticlockwise in-plane microvortices are generated in order to break laminar flows in the microfluidic channel and function as a micromixer. To enhance the mixing efficiency, the electrodes were rotated at various angles (θ). We set up a numerical model and design a perfusion chip integrated with a 6-pair electrode micromixer to research the mixing efficiency of three types of micromixers ($\theta = 0^\circ$, 30° , and 60°). The mixing efficiency is displayed by grayscale images in the numerical model and fluorescein solution images in the experiment. The applicability of our micromixer was demonstrated by culturing human breast cancer cells (MCF-7) and performance of a concentration gradient drug (tamoxifen) test of MCF-7 in the chip. The Y-shaped channels imitate the fluids from two organs, and the mixing area imitates the part of microfluidic channel network, which represents a typical simplified model of drug screening in an organs-on-a-chip system.

II. ACET THEORY

The ACET effect arises from the interaction of non-uniform electric fields and uniform temperature (i.e., temperature gradient) in the microfluid. The non-uniform electric field is applied to the fluid to generate Joule heating³⁷ and subsequently induce the temperature gradient. The electric properties of the fluid, such as conductivity and permittivity, were changed by the temperature gradient, which further induced free charges. Free charges move in the non-uniform electric field, which exerts body force on the fluid to generate ACET flow.³²

When an electric field distribution occurs throughout the fluid region, Joule heating of the fluid can be expressed by the energy balance equation^{36,38}

$$k\nabla^2 T + \frac{1}{2}\langle\sigma\mathbf{E}^2\rangle = 0, \quad (1)$$

where T is the temperature of the fluid, \mathbf{E} is the applied electric field, and σ and k are the electrical and thermal conductivities of the fluid. The electric field in the fluid can be determined by the Laplace equation³⁹

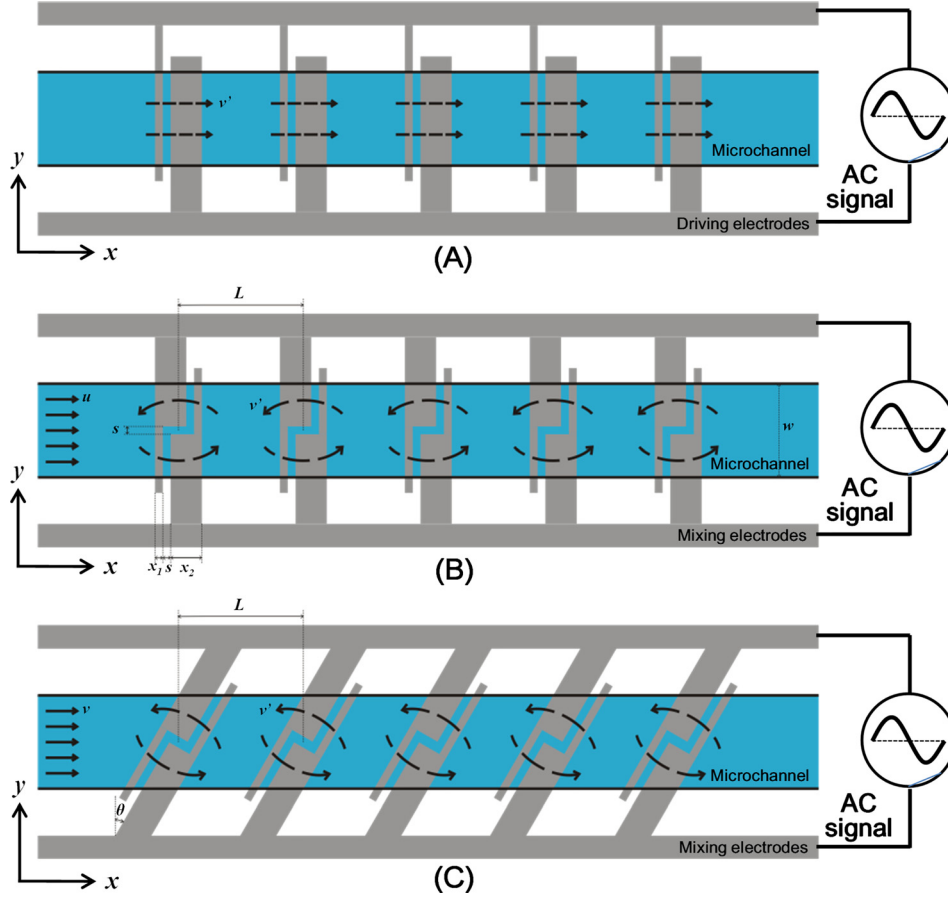


FIG. 1. Schematic diagram of the ACET pump and mixer. (a) ACET pump based on the asymmetric electrode array. (b) and (c) ACET mixer based on compound asymmetric electrode generating in-plane microvortices.

$$\nabla V^2 = 0, \quad (2)$$

where V denotes the root-mean-square voltage, and $\mathbf{E} = -\nabla V$.

The resultant time averaged electrothermal force ($\langle \mathbf{F}_{et} \rangle$) can be calculated as⁴⁰

$$\langle \mathbf{F}_{et} \rangle = \frac{1}{2} \cdot \frac{\varepsilon(\alpha - \beta)}{1 + (2\pi f \varepsilon / \sigma)^2} - \frac{1}{4} \cdot \varepsilon \alpha |\mathbf{E}|^2 \nabla T, \quad (3)$$

where f is the frequency of the AC electro field, $\alpha = -0.004(\text{K}^{-1})$ and $\beta = 0.02(\text{K}^{-1})$.⁴¹

Navier-Stokes equation is applied for an incompressible fluid of low Reynolds number, and the steady fluid flow can be described as below⁴²

$$-\nabla p + \eta \nabla^2 \mathbf{u} + \langle \mathbf{F}_{et} \rangle = 0, \quad \nabla \cdot \mathbf{u} = 0, \quad (4)$$

where \mathbf{u} is the fluid velocity vector, p is the pressure, and η denotes the dynamic viscosity.

III. MATERIALS AND METHODS

A. Design and fabrication of micromixer

Fig. 2(a) shows the design of the micromixer. The micromixer used in this study consists of a Polydimethylsiloxane (PDMS) Y-shaped microchannel (0.5 mm width, 100 μm height) with 6 pairs of indium-tin-oxide (ITO) microelectrodes and a cell culture chamber (10 mm diameter,

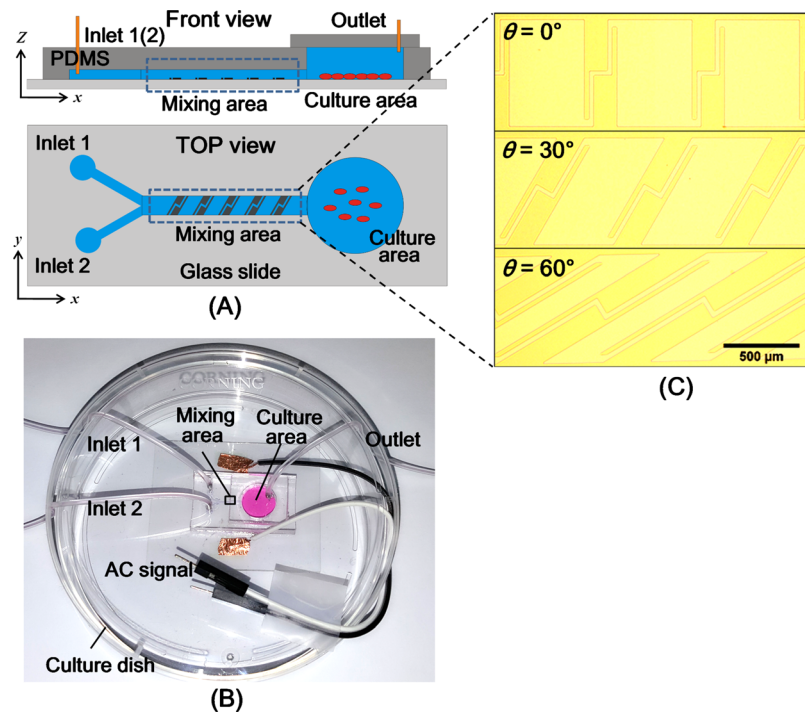


FIG. 2. Design of the device. (a) Schematic, (b) the fabricated micromixer, and (c) the electrodes in microscopic views.

3 mm height). The length of the mixing area is <7 mm (Fig. 2(b)). The mixing electrodes were $0.2 \mu\text{m}$ (200 nm) thick, and $30 \mu\text{m}/150 \mu\text{m}$ wide, distributed with a $30 \mu\text{m}$ in-pair separation and $700 \mu\text{m}$ between-pair center-to-center distance (L in Fig. 1(c)). The rotation angles of electrodes in the mixing area are 0° , 30° , and 60° (Fig. 2(c)).

The glass slide with ITO electrodes was fabricated using photolithography, and the PDMS layer was produced using a conventional soft-lithography procedure (Fig. 3). Microfabrication of the glass slide with ITO electrodes required the following steps. First, the ITO glass slide was washed in acetone, alcohol, and deionized water, respectively, for 15 min each using an ultrasonic cleaner. After drying in the oven at 120°C , the positive photoresist (AZ4620, Ruicai) was spun in ITO glass (ITO8008, Kaivo) by a spin coater at 500 rpm for 18 s and then at

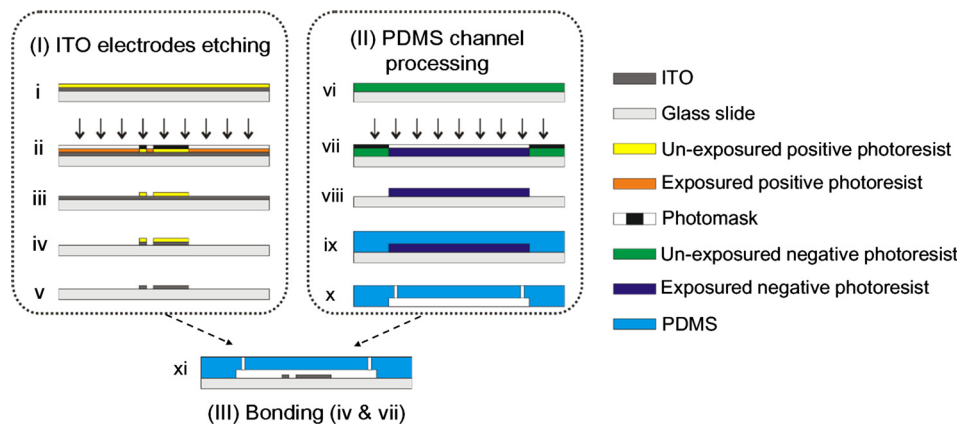


FIG. 3. Fabrication process of (I) etching electrode in lithography, (II) casting PDMS channel, and (III) bonding. (i) Spin coat positive photoresist on the surface of ITO glass. (ii–iii) Photoresist was selectively exposed by photomask and developed. (iv–v) Etch with HCl and strip off the photoresist using acetone. (vi) Laminate negative dry film photoresist onto the glass slide. (vii–viii) Photoresist was selectively exposed by photomask and developed. (ix–x) Poured and cured PDMS, and then punch holes. (xi) PDMS channel was bonded to glass slide with ITO electrodes.

3200 rpm for 60 s. The ITO coated photoresist was then heated for 6 min after being positioned on a level hot plate (EH35B, LabTech) set at 100 °C. Next, the photoresist was selectively exposed by a photomask designed with an AutoCAD software (Autodesk). Following exposure, the photoresist was placed on a hot plate heated to 110 °C for 6 min. Subsequently, the photoresist subject to exposure was developed in 2.38% tetramethyl ammonium hydroxide solution (50605816, TOK Co.) for 4 min. The ITO glass slide with the patterned photomask was then soaked in 20% HCl for 30 min. Finally, the photoresist was stripped using acetone. Three sheets of the dry film photoresist (RistonSD238, Dupont) were used to fabricate the PDMS mold layer through a lamination process on top of a glass slide. The photoresist was then selectively exposed by a photomask and developed in 1 wt. % Na₂CO₃ solution. The PDMS curing agent was combined with the elastomer base (DOW Corning) at a ratio of 10:1 (w/w) to create a mixture that was then applied to the exposed photoresist mold and dried through degassing in a vacuum chamber for 30 min. The PDMS mixture was then baked in an oven for 60 min at 80 °C to allow curing. An oxygen plasma (ZEPTO, Diener) treatment was used to bond the glass slide housing the ITO electrodes to the PDMS layer after the alignment of the two components. Lastly, the chip was immersed in 70% ethanol for 45 min and then subject to UV irradiation for 45 min to achieve sterilization prior to culturing cells.

B. Evaluation of mixing efficiency

The electrical conductivity of culture medium primarily depends on chloride saline solution. Therefore, aqueous KCl solutions with the same conductivity as the culture medium were utilized to evaluate the mixing efficiency of the micromixer. Fluorescein (Kermel) was used as fluorescent dye to enable visualization of the mixing process. To demonstrate the mixing efficiency of the micromixer with rotation angles of 0°, 30°, and 60°, the aqueous KCl solution and the fluorescent dye solution (20 μM) in aqueous KCl solution were introduced into the Y-shaped microchannel with a two-port syringe pump (PHD ULTRA, Harvard Apparatus). The perfusion flow rate of each syringe was maintained at 10.417 μl/h (250 μl/day), so the total flow rate in the microchannel was 20.833 μl/h (500 μl/day). The function generator (TGA12104, TTI) was used to apply AC peak voltages of 2.5, 3, 3.5, and 4 V at a frequency of 500 kHz on the electrodes and adjusted with an oscilloscope (TDS2024, Tektronix). The phase difference of signal on a pair of electrodes was π . The mixing process was captured under a fluorescent microscope (BX53, Olympus) that was focused 50 μm above the bottom of the glass surface to acquire images.

C. Cells, culture medium, and measurement of electrical conductivity of medium

The ATCC acquired line of cells known as Michigan Cancer Foundation-7 (MCF-7) was from human breast tumor. A medium of RPMI 1640 (11875, ThermoFisher) supplemented with 10% fetal bovine serum (FBS) (16000, ThermoFisher), as well as 1% penicillin/streptomycin (155140, ThermoFisher), was used to maintain cells. Tamoxifen (TAM) was obtained from Sigma.

The culture medium (RPMI 1640, 10% FBS, 1% P/S) with tamoxifen was used in our study to investigate the induced death of MCF-7. The electrical conductivity of medium samples with 0, 1.25, 2.5, and 5 μM TAM was tested using a commercial conductivity sensor (DDSJ-308A, Leici), respectively.

D. Culture MCF-7 and tamoxifen-induced rapid death of MCF-7 in the device

Cell suspensions (3.33×10^5 /ml) were injected from the exit point of the device through the cell culture chamber in order to fill the culture chamber by a syringe. As a result, the density of the cells was found to be 10^5 /cm². The device with the syringe was gently placed in the incubator for a time period of 4 h for cell attachment. Following this period, the syringe at the outlet was removed, and the culture medium without tamoxifen in two syringes was introduced into the Y-shaped microchannel with a syringe pump at the flow rate of 10.417 μl/h each. After the device was returned to the incubator, the AC function generator was activated at the peak

voltage of 3 V and a frequency of 500 kHz. The perfusion culture cells then lasted for 5 days. For control and comparison, cells were seeded at the same concentration in 48-well plates (CLS3338, Corning), and the medium was replaced with 500 μl once each 24 h period. These tests were carried out in three replicates.

For the experiment of accelerated MCF-7 death prompted by the presence of tamoxifen in the device, the groups of experiments are shown in Table I. All the groups seed the MCF-7 cells at the same density as above. The perfusion flow rate of each syringe was maintained at 10.417 $\mu\text{l}/\text{h}$, and the micromixer was operated at the peak voltage of 3 V and a frequency of 500 kHz by the AC function generator. The experiment of tamoxifen-induced rapid death lasted for 5 days, and the experiments were conducted in three replicates.

E. Cell viability and cell proliferation

The Live/Dead[®] Viability Kit (L-3224, ThermoFisher)⁴³ was used to evaluate the viability of cells. Calcein AM and ethidium homodimer-1 were first diluted in Dulbecco phosphate-buffered saline (DPBS) at concentrations of 0.5 $\mu\text{l}/\text{ml}$ and 2 $\mu\text{l}/\text{ml}$, respectively. At 1, 3, and 5 days, samples were washed 3 times in DPBS and incubated in the mixture for 15 min at 37 °C. All samples were imaged immediately without mounting using a fluorescence microscope (IX2-UCB, Olympus).

Cell proliferation was evaluated using PicoGreen[®] DNA quantification assay (P7589, ThermoFisher). At each time point (0, 1, 3, and 5 days) of the cyto-toxicity test, the samples were, respectively, lysed for 2 h with 500 μl of 50 $\mu\text{g}/\text{ml}$ proteinase *k* at 37 °C. The samples were subsequently pelleted via centrifugation for a period of 10 min at 18 000 rpm and 4 °C. Next, the samples were incubated in the dark with PicoGreen[®] working solution (1:200 dilution) for 5 min at room temperature. At the excitation wavelength of 485 nm, and the emission wavelength of 520 nm, the fluorescence of samples in 96-well plates was tested using a microplate reader (Fluostar). The standard curve was created by mixing 100 μl of each sample concentration (2 μM , 200 nM, 20 nM, 2 nM, and 0 nM) with 100 μl PicoGreen[®] solution (1:200) in a 96-well plate and incubating at room temperature for 5 min. The fluorescence measurement of the standard curve mixture has been previously described.

IV. NUMERICAL MODEL

A. Numerical setups

Mathematical simulations were performed using COMSOL Multiphysics 5.1 (Comsol, Inc.) to evaluate the mixing efficiency of the micromixer with three types of electrode arrays. A 3D model of the same size as the mixing area of the experimental device was established. Appropriate electrostatics, heat transfer, laminal flow, and transport of diluted species modules were chosen to solve the equations for electric, thermal, velocity, and convective-diffusion equations, respectively. Fig. 4 indicates the boundary conditions of electrical, thermal, and fluidic settings, and the schematic was not drawn to scale. The concentrations of two different fluids to be mixed are set as $C=0 \text{ mol}/\text{m}^3$ and $C=1 \text{ mol}/\text{m}^3$ at inlet 1 and inlet 2, respectively. Three types of micromixers (electrodes with rotation angles of 0°, 30°, and 60°) were then individually calculated. Specific parameters used in the numerical study are shown in Table II.

TABLE I. The groups of MCF-7 tamoxifen-induced rapid death experiments.

Group no.	Inlet 1	Inlet 2
1	5 μM tamoxifen in RPMI 1640	5 μM tamoxifen in RPMI 1640
2	5 μM tamoxifen in RPMI 1640	RPMI 1640
3	2.5 μM tamoxifen in RPMI 1640	RPMI 1640
Ctrl	RPMI 1640	RPMI 1640

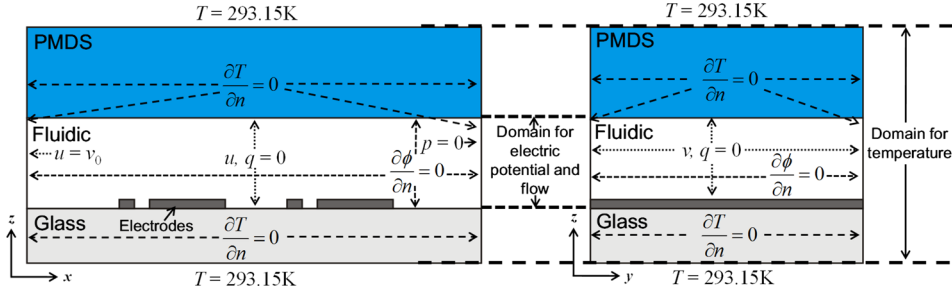


FIG. 4. Boundary conditions of the simulation, where T is the temperature, p is the pressure, ϕ is the electric potential, and u , v , and q indicate the velocity of the fluid in the x , y , and z directions, respectively.

B. Simulation results

Fig. 5 compares the mixing characteristics of the micromixer of three types at the peak voltage of 3 V and a frequency of 500 kHz. The mixing performance in each type of micromixer improves as the number of electrode pairs increases. Evidently, the mixing performance is also enhanced with an increased rotation angle. The performance of the mixing is evaluated with the following equation:

$$\eta_m = \left[1 - \sqrt{\frac{1}{n-1} \sum_{i=1}^n \left(\frac{I_i - I_{ave}}{I_{ave}} \right)^2} \right] \times 100\%, \quad (5)$$

where η_m , n , I_i , and I_{ave} are the mixing efficiency, the total number of pixels, the intensity at pixel i , and the average intensity of total pixels. Generally, the value of η_m equal to 90% was considered complete mixing.³⁰

Fig. 5(b) compares the mixing efficiencies of the three types of micromixers calculated by Equation (5) with the applied peak voltage ranging from 0 to 4 V at the outlet of the mixing area ($x = 4.5$ mm). The mixing efficiencies of the three types of micromixers increased with the growth of voltage. The value η_m of the micromixer of $\theta = 60^\circ$ is over 90% at the voltages above 3 V, whereas it was over 90% only at 4 V for the micromixer of $\theta = 30^\circ$. The mixing

TABLE II. Property values used in the numerical study.

Property	Value	Property	Value
Height of the microchannel	100 μm	Width of the microchannel	500 μm
Width of the wide part of the electrode	150 μm	Width of the narrow part of the electrode	30 μm
Gap between in-pair electrodes	30 μm	Electrode pairs center-to-center distance	700 μm
Electrode pairs	6	Rotation angles of electrodes	$0^\circ, 30^\circ, 60^\circ$
Thickness of the glass slide	0.4 mm	Thickness of PDMS	2 mm
Amplitude of the drive voltage	0.5–4 V	Phase difference of signal on a pair of electrodes	π
Frequency	500 kHz	Fluid conductivity	1.7 S/m
Thermal conductivity of the fluid sample	0.6 W/mK (Ref. 44)	Thermal conductivity of the glass slide	1.1 W/mK (Ref. 36)
Thermal conductivity of fluid PDMS	0.2 W/mK (Ref. 45)	Ambient/reference temperature	310.15 K
Mass density of the fluid sample	0.96 g/ml (Ref. 46)	Dynamic viscosity at reference temperature	0.89 mPa s (Ref. 46)
Velocity of inflow	115.74 $\mu\text{m/s}$	Diffusion coefficient	2.4×10^{-11} m^2/s (Ref. 47)

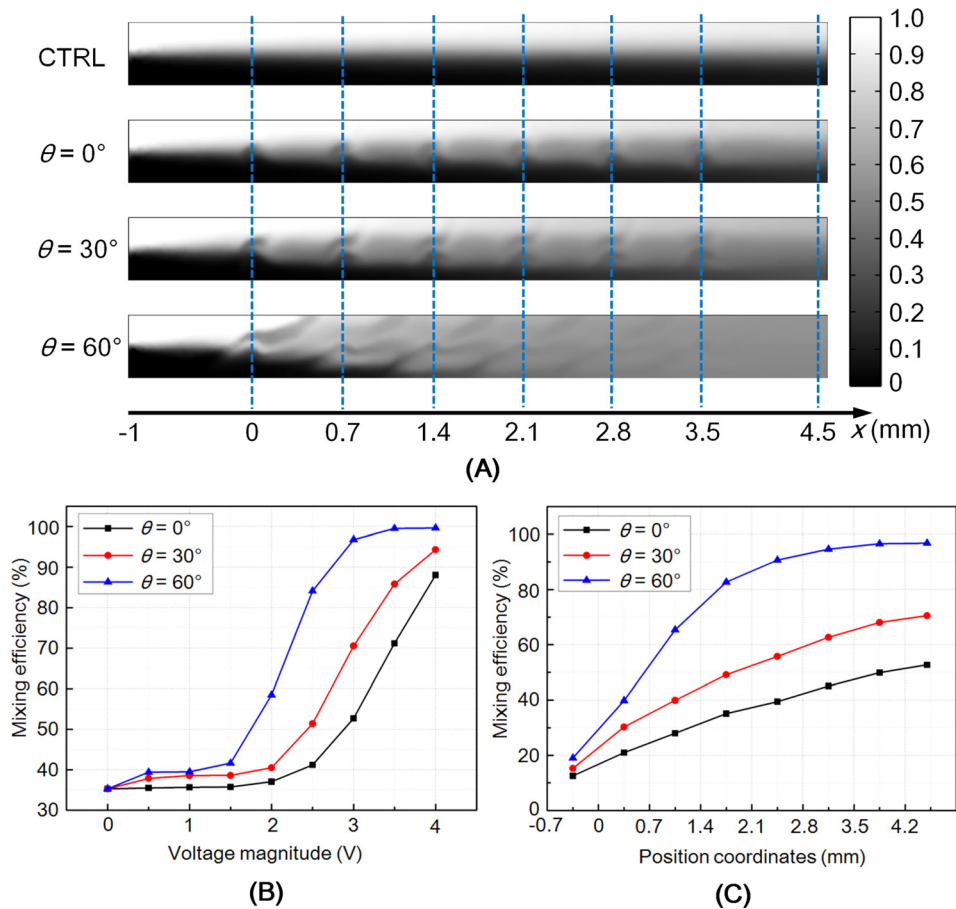


FIG. 5. Comparison of simulation results among $\theta = 0^\circ$, 30° , and 60° . (a) Grayscale images of the simulated results. The blue dashed lines indicate the x positions of the centers of in-pair electrodes. The pure white denotes the concentration of 1 mol/m^3 , whereas the pure black indicates the concentration of 0 mol/m^3 . (b)–(c) Comparison of the mixing efficiencies at different (b) applied voltages and (c) positions.

efficiencies of the micromixer with straight electrodes ($\theta = 0^\circ$) were less than 90% at the voltages ranging from 0 to 4 V. Fig. 5(c) depicts the mixing efficiencies of the three types of micromixers in different locations at the peak voltage of 3 V. The mixing efficiency of the micromixer of $\theta = 60^\circ$ was 90.66% when mixed by only 4 pairs of electrodes ($x = 2.45 \text{ mm}$). Meanwhile, the mixing efficiencies were 49.88% ($\theta = 0^\circ$) and 68.06% ($\theta = 30^\circ$) when mixed by 6 pairs of electrodes ($x = 3.85 \text{ mm}$). Therefore, the mixing performance of the micromixer with $\theta = 60^\circ$ is far better than that of $\theta = 0^\circ$ and $\theta = 30^\circ$.

V. RESULTS AND DISCUSSIONS

A. Electrical conductivity detection of medium

Electrical conductivity is one of the key factors to ACET flow, which affects the velocity of ACET flow and the mixing efficiency of the micromixer. Therefore, the electrical conductivities of culture medium with different tamoxifen concentrations were measured (Table III). The concentration of salt ions (e.g., chloridion, sodion, calcium, etc.) affects the electrical conductivity of the medium. As low concentrations of tamoxifen melt in the medium, there is only a miniscule change in the electrical conductivity of the culture medium. The measured conductivity of the culture medium (RPMI 1640 with 10% FBS and 1% P/S) with low concentrations of tamoxifen was maintained at $\sim 1.7 \text{ S/m}$.

TABLE III. Results of the conductivity of RPMI 1640 with tamoxifen.

Medium	Electric conductivity (S/m)
RPMI 1640 (10% FBS, 1% P/S)	1.688 ± 0.013
1.25 μM tamoxifen in RPMI 1640 (10% FBS, 1% P/S)	1.696 ± 0.018
2.50 μM tamoxifen in RPMI 1640 (10% FBS, 1% P/S)	1.698 ± 0.019
5.00 μM tamoxifen in RPMI 1640 (10% FBS, 1% P/S)	1.701 ± 0.016

B. Mixing efficiency

Fig. 6(a) shows the mixing results of typical fluorescence images, in which aqueous KCl solution and the fluorescent dye solution (20 μM) in aqueous KCl solution were introduced into the Y-shaped channel at 10.417 $\mu\text{l/h}$ each. As a result, the mean velocity was calculated to be 115.74 $\mu\text{m/s}$. The mixing performance is found to be enhanced as the rotation angle increases, which is in accordance with the simulation result depicted in Fig. 5. The fluorescence is slightly uneven at the joint position of two images (red line) because of instability from the low flow rate of the fluid. Experimental results of the mixing efficiencies of three types of micromixers at different applied voltages are shown in Fig. 6(b). Mixing efficiency improves with increasing voltage and the increasing rotation angle of electrodes. The mixing efficiencies of micromixers of $\theta = 0^\circ$, 30° , and 60° were found to be 76.22%, 83.28%, and 92.37%, respectively, at 4 V. Complete mixing was achieved only by micromixers of $\theta = 60^\circ$. The mixing efficiencies of micromixers of $\theta = 60^\circ$ were 89.12% (approximate complete mixing) at 3 V. In view of the

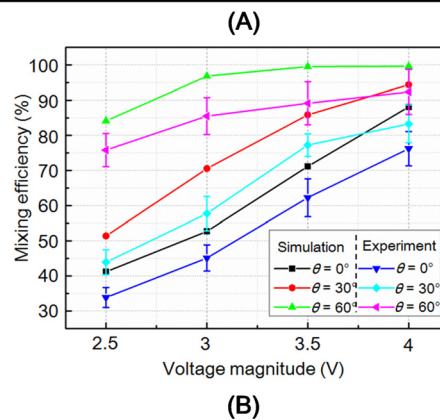
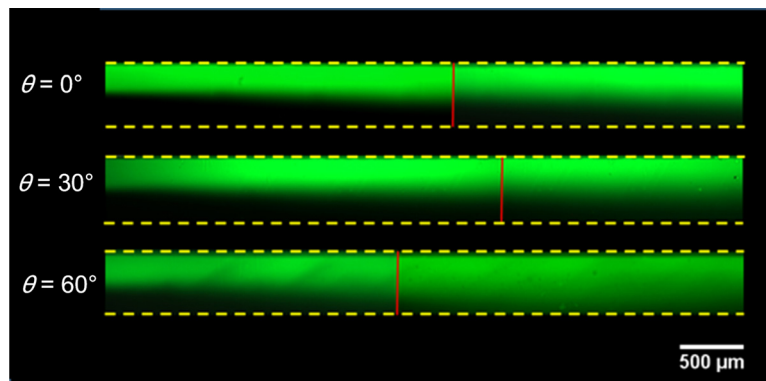


FIG. 6. Comparison of the experimental mixing results of three types of micromixers at a fluid velocity of 115.74 $\mu\text{m/s}$. (a) Fluorescence micrographs of mixing results of three types of micromixers at the voltage of 3 V. The yellow dotted lines denote the boundaries of the channel, and the red lines depict the joint positions of two images. (b) Experimental and simulated results for mixing efficiencies of three types of micromixers at different applied voltages.

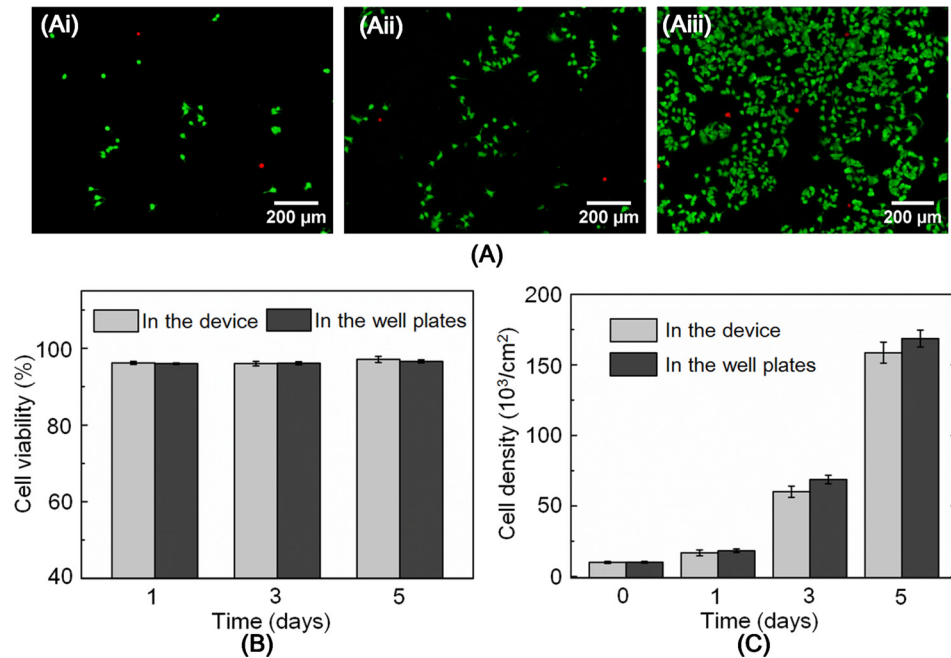


FIG. 7. Results of perfusion culture of cells without tamoxifen. (a) Fluorescent images of MCF-7 perfusion cultured in the device at (a-i) 1, (a-ii) 3, and (a-iii) 5 days. Green depicts living cells, while cells that have died are depicted with red. (b) Statistical results of cell viability of MCF-7 cultured in the device at 1, 3, and 5 days. (c) Statistical outcomes of MCF-7 proliferation cultured in the device at 1, 3, and 5 days.

more Joule heating was generated in high voltage, the voltage of 3 V could be applied to the drug induced death of tumor cells.

Fig. 6(b) also shows a comparison of the experimental and simulated mixing results. Obviously, mixing efficiencies in simulation were higher than those of the results from the experiments conducted with the same conditions. The reason for the difference in mixing efficiencies between the experimental and simulated results is the inevitable model error of the ACET flow. The actual voltage drop on the electrodes caused by numerous electrode pairs and electrochemical reactions on electrodes will change with applied voltages. Moreover, buoyancy force that reduces the velocity of ACET flow was omitted to simplify the calculation in our simulation,³⁵ even though it exists in experiments.

C. Cell culture and drug test in the device

The mixing efficiency is evaluated with the help of the numerical model and mixing experiment. Further study is required to determine whether the micromixer can be successfully integrated into three organs-on-a-chip systems. The organs-on-a-chip system is a complex system which integrated with multi-organ chips. It is impractical to run our micromixer in the organs-on-a-chip, but in a chip for the drug test. MCF-7 and tamoxifen, that is, the model cells and their killer drug, were used to perform the applicability of our micromixer.

Temperature changes in the fluid and parameters of the electric field are the key factors in this model as the mechanism of the micromixer is based on electrothermal flow. Moreover, excessive temperature or electric field conditions will damage cells. Consequently, verification testing of these conditions is required to determine if the environment is in a reasonable range for cell culture. This analysis is of paramount importance for applications with drugs. The culture medium RPMI 1640 without tamoxifen was introduced into the microchannel both in inlet 1 and inlet 2 using the syringe pump while the micromixer was activated by the signal generator.

To confirm the feasibility of our micromixer, MCF-7 cells were used as model cells, while tamoxifen was used to test their rapidly induced death. MCF-7 cells were dynamically

cultured in the active micromixer for 5 days. The culture results of perfusion culturing cells without tamoxifen are shown in Fig. 7. Fig. 7(a) shows fluorescent staining of MCF-7 perfusion cultured in the micromixer at 1 (Fig. 7(a-i)), 3 (Fig. 7(a-ii)), and 5 (Fig. 7(a-iii)) days. The green dots represent live cells, and the red dots indicate dead cells. The cells are distributed uniformly, and a small number appears dead at each time point. Figs. 7(b) and 7(c) display the statistical viability and proliferation outcome of the MCF-7 cells cultured in the device and in the 48-well plates. The data show that the cells grew well in both devices and the 48-well plates over 5 days. The quantified viabilities of MCF-7 were observed at over 95% at each time point in both conditions. The quantified viability of MCF-7 in the device is found to be slightly higher than that in the chip due to the shear stress from the fluid, resulting in the removal of dead cells. However, the cell proliferation rate of MCF-7 in the device was found to be lower than that in the chip. This may be because the cells prefer a static environment to a dynamic environment (i.e., device) as the cells may experience certain shear stress and need to adapt themselves to the environment although the difference was not significant.³² As the cells cultured grew well in the device, the cells were not damaged by the electric field or ACET flow in the device. Consequently, drug testing can be studied in the device without interference from the electric field or the ACET flow.

Fig. 8(a) shows the live/dead fluorescent staining results of MCF-7 with 1.25 μM and 2.50 μM tamoxifen in the device after culture for 1, 3, and 5 days. Compared with the culture results of MCF-7 without tamoxifen (Fig. 7(a)), the number and viability of cells cultured with

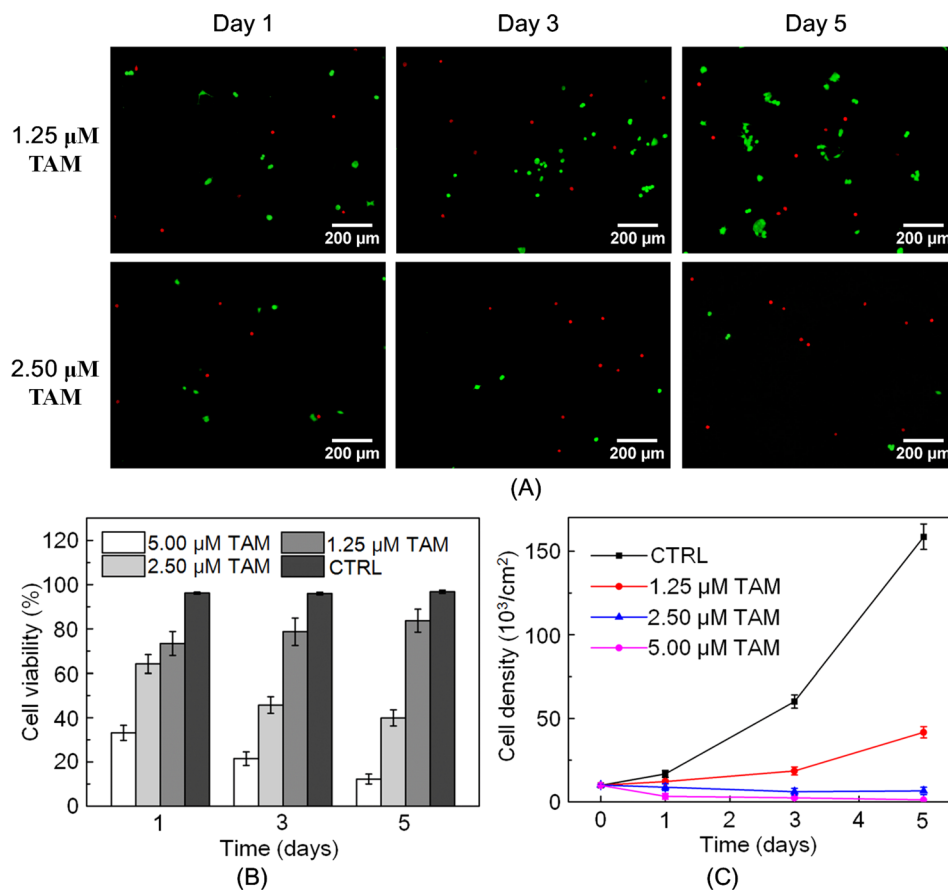


FIG. 8. Results of perfusion culturing cells with multiple concentrations of tamoxifen. (a) Fluorescent images of MCF-7 with 1.25 μM and 2.50 μM tamoxifen in the device after culture for 1, 3, and 5 days. Green depicts living cells, while cells that have died are depicted with red. (b) Statistical results of cell viability of MCF-7 cultured with multiple concentrations of tamoxifen in the device at 1, 3, and 5 days. (c) Statistical outcomes of MCF-7 proliferation cultured with multiple concentrations of tamoxifen in the device at 1, 3, and 5 days.

multiple concentrations of tamoxifen were noticeably less at each time point. Furthermore, with tamoxifen concentration increase, the proportion of viable cells reduces significantly at 1, 3, and 5 days. Fig. 8(b) presents the statistical results of cell viability of MCF-7 cultured with multiple concentrations of tamoxifen in the device at each time point. In the control groups, the viability of MCF-7 was over 96%. The viability of cells cultured at the tamoxifen concentration of 1.25 μM increases slightly from day 1 to day 5, whereas the viability of cells cultured at the tamoxifen concentration of 2.5 μM and 5 μM is found to decrease over the same time period. Fig. 8(c) shows the statistical results of MCF-7 proliferation cultured with multiple concentrations of tamoxifen. Compared with the control group (0 μM tamoxifen), cell proliferation is significantly inhibited by multiple concentrations of tamoxifen. Negative growth of the number of cells occurred in 2.5 μM and 5 μM tamoxifen and low growth in tamoxifen with 1.25 μM . Only a few cells were alive with 5 μM tamoxifen application from day one, which presents the ability of tamoxifen to rapidly induce the death of MCF-7.

VI. CONCLUSIONS

This paper introduces ACET as a novel mixing approach for cell culture and drug testing applications. We have demonstrated three types of micromixers with different rotation angles (0°, 30°, and 60°), which generated observably different in-plane microvortices of ACET flow, thus showing different mixing performances. The mixing performance was enhanced with a greater rotation angle and increased applied voltage. From the numerical and experimental results, the novel recombined ACET asymmetric electrodes with rotating angles of 60° exhibited prominent high mixing efficiency towards the fluid with high conductivity. The mixing efficiency in our micromixer was 89.12% (approximate complete mixing) at a voltage of 3 V and a frequency of 500 kHz, which was effective for the drug testing conducted with tumor cells. Satisfactory performance of our micromixer was demonstrated by successful application of multiple concentrations of tamoxifen induced rapid death of MCF-7 for 5 days, which shows great potential of the ACET micromixer for organs-on-a-chip systems.

ACKNOWLEDGMENTS

This work was supported by the National Natural Science Foundation of China (Nos. 51305106 and 11372093), Self-Planned Task (Nos. 201510B and SKLRS201606C) of State Key Laboratory of Robotics and System (HIT), the Programme of Introducing Talents of Discipline to Universities (No. B07018), and the start-up fund from Interdisciplinary Division of Biomedical Engineering, the Hong Kong Polytechnic University.

- ¹S. V. Murphy and A. Atala, *Nat. Biotechnol.* **32**(8), 773 (2014).
- ²N. S. Bhise, V. Manoharan, S. Massa, A. Tamayol, M. Ghaderi, M. Miscuglio, Q. Lang, Y. Shrike Zhang, S. R. Shin, G. Calzone, N. Annabi, T. D. Shupe, C. E. Bishop, A. Atala, M. R. Dokmeci, and A. Khademhosseini, *Biofabrication* **8**(1), 014101 (2016).
- ³P. Neuzi, S. Giselbrecht, K. Länge, T. J. Huang, and A. Manz, *Nat. Rev. Drug Discovery* **11**(8), 620 (2012).
- ⁴X. Zhao, S. Liu, L. Yildirim, H. Zhao, R. Ding, H. Wang, W. Cui, and D. Weitz, *Adv. Funct. Mater.* **26**(17), 2809 (2016).
- ⁵Q. Lang, Y. Ren, Y. Wu, Y. Guo, X. Zhao, Y. Tao, J. Liu, H. Zhao, L. Lei, and H. Jiang, *RSC Adv.* **6**(32), 27183 (2016).
- ⁶D. Huh, G. A. Hamilton, and D. E. Ingber, *Trends Cell Biol.* **21**(12), 745 (2011).
- ⁷J. P. Wikswo, E. L. Curtis, Z. E. Egleton, B. C. Evans, A. Kole, L. H. Hofmeister, and W. J. Matloff, *Lab Chip* **13**(18), 3496 (2013).
- ⁸C. Moraes, J. M. Labuz, B. M. Leung, M. Inoue, T. H. Chun, and S. Takayama, *Integr. Biol.* **5**(9), 1149 (2013).
- ⁹J. P. Wikswo, F. E. Block, D. E. Cliffel, C. R. Goodwin, C. C. Marasco, D. A. Markov, D. L. McLean, J. A. McLean, J. R. McKenzie, and R. S. Reiserer, *IEEE Trans. Biomed. Eng.* **60**(3), 682 (2013).
- ¹⁰R. Verma, R. R. Adhikary, and R. Banerjee, *Lab Chip* **16**(11), 1978 (2016).
- ¹¹V. Hessel, H. Löwe, and F. Schönfeld, *Chem. Eng. Sci.* **60**(8–9), 2479 (2005).
- ¹²C. Y. Lee, W. T. Wang, C. C. Liu, and L. M. Fu, *Chem. Eng. J.* **288**, 146 (2016).
- ¹³Y. Wang, Q. Lin, and T. Mukherjee, *Lab Chip* **5**(8), 877 (2005).
- ¹⁴Y. K. Suh and S. Kang, *Micromachines* **1**(3), 82 (2010).
- ¹⁵C. Y. Lee, C. L. Chang, Y. N. Wang, and L. M. Fu, *Int. J. Mol. Sci.* **12**(5), 3263 (2011).
- ¹⁶W. Buchegger, C. Wagner, B. Lendl, M. Kraft, and M. J. Vellekoop, *Microfluid. Nanofluid.* **10**(4), 889 (2011).
- ¹⁷T. Tofteberg, M. Skolimowski, E. Andreassen, and O. Geschke, *Microfluid. Nanofluid.* **8**(2), 209 (2010).
- ¹⁸X. Feng, Y. Ren, and H. Jiang, *Biomicrofluidics* **8**(3), 034106 (2014).

- ¹⁹X. Feng, Y. Ren, and H. Jiang, *Biomicrofluidics* **7**(5), 54121 (2013).
- ²⁰P. Paik, V. K. Pamula, and R. B. Fair, *Lab Chip* **3**(4), 253 (2003).
- ²¹X. Guan, L. Hou, Y. Ren, X. Deng, Q. Lang, Y. Jia, Q. Hu, Y. Tao, J. Liu, and H. Jiang, *Biomicrofluidics* **10**(3), 034111 (2016).
- ²²N. Sasaki, T. Kitamori, and H. B. Kim, *Lab Chip* **6**(4), 550 (2006).
- ²³N. Sasaki, T. Kitamori, and H. B. Kim, *Electrophoresis* **33**(17), 2668 (2012).
- ²⁴Q. Cao, X. Han, and L. Li, *Int. J. Appl. Electrom.* **47**(3), 583 (2015).
- ²⁵M. C. Jo and R. Guldiken, *Sens. Actuator, A* **196**, 1 (2013).
- ²⁶W. Liu, Y. Ren, J. Shao, H. Jiang, and Y. Ding, *J. Phys. D: Appl. Phys.* **47**(7), 075501 (2014).
- ²⁷Y. Ren, J. Liu, W. Liu, Q. Lang, Y. Tao, Q. Hu, L. Hou, and H. Jiang, *Lab Chip* **16**(15), 2802 (2016).
- ²⁸Y. Jia, Y. Ren, and H. Jiang, *Electrophoresis* **36**(15), 1744 (2015).
- ²⁹N. G. Green, A. Ramos, A. González, H. Morgan, and A. Castellanos, *Phys. Rev. E* **61**(4), 4011 (2000).
- ³⁰S. H. Huang, S. K. Wang, H. S. Khoo, and F. G. Tseng, *Sens. Actuator, B* **125**(1), 326 (2007).
- ³¹N. G. Green, A. Ramos, A. Gonzalez, A. Castellanos, and H. Morgan, *J. Electrostat.* **53**(2), 71 (2001).
- ³²J. Wu, M. Lian, and K. Yang, *Appl. Phys. Lett.* **90**(23), 234103 (2007).
- ³³W. Y. Ng, S. Goh, Y. C. Lam, C. Yang, and I. Rodriguez, *Lab Chip* **9**(6), 802 (2009).
- ³⁴Y. Wu, Y. Ren, and H. Jiang, "Enhanced model-based design of a high-throughput three dimensional micromixer driven by alternating-current electrothermal flow," *Electrophoresis* (to be published).
- ³⁵Q. Lang, Y. Wu, Y. Ren, Y. Tao, L. Lei, and H. Jiang, *ACS Appl. Mater. Interfaces* **7**(48), 26792 (2015).
- ³⁶A. Salari, M. Navi, and C. Dalton, *Biomicrofluidics* **9**(1), 014113 (2015).
- ³⁷P. S. Gupta and A. S. Gupta, *Can. J. Chem. Eng.* **55**(6), 744 (1977).
- ³⁸A. Ramos, H. Morgan, N. G. Green, and A. Castellanos, *J. Phys. D: Appl. Phys.* **31**(18), 2338 (1998).
- ³⁹L. Onsager, *J. Am. Chem. Soc.* **58**(8), 1486 (1936).
- ⁴⁰D. F. Chen and H. Du, *J. Micromech. Microeng.* **16**(11), 2411 (2006).
- ⁴¹X. Xuan, *Electrophoresis* **29**(1), 33 (2008).
- ⁴²J. D. Cole, *Quart. Appl. Math.* **9**(3), 225 (1951).
- ⁴³X. Zhao, Q. Lang, L. Yildirimer, Z. Y. Lin, W. Cui, N. Annabi, K. W. Ng, M. R. Dokmeci, A. M. Ghaemmaghami, and A. Khademhosseini, *Adv. Healthcare Mater.* **5**(1), 108 (2016).
- ⁴⁴A. O. Govorov, W. Zhang, T. Skeini, H. Richardson, J. Lee, and N. A. Kotov, *Nanoscale Res. Lett.* **1**(1), 84 (2006).
- ⁴⁵X. Xuan, B. Xu, D. Sinton, and D. Li, *Lab Chip* **4**(3), 230 (2004).
- ⁴⁶L. D. Garza-García, E. García-López, S. Camacho-León, M. R. Rocha-Pizaña, F. López-Pacheco, J. López-Meza, D. Araiz-Hernández, E. J. Tapia-Mejía, G. T. Santiago, and C. A. Rodríguez-González, *Lab Chip* **14**(7), 1320 (2014).
- ⁴⁷E. Guiot, M. Enescu, B. Arrio, G. Johannin, G. Roger, S. Tostí, F. Tfibel, F. Mérola, A. Brun, and P. Georges, *J. Fluoresc.* **10**(4), 413 (2000).